Supplementary Material

Structure Retention of Silica Gel-Encapsulated Bacteriorhodopsin in Purple Membrane and in Lipid Nanodiscs

Sukriti Gakhar[‡], Subhash H. Risbud[†], and Marjorie L. Longo*[,‡]

[‡]Department of Chemical Engineering, University of California Davis, Davis, California 95616, United States

[†]Department of Materials Science and Engineering, University of California Davis, Davis, California 95616, United States

*E-mail: mllongo@ucdavis.edu

(12 pages total, 7 figures, 0 tables)

Table of Contents:

S1. Materials and Methods

Materials. Bacteriorhodopsin (BR) was purchased in the form of lyophilized Purple Membrane (PM) from Bras del Port S.A. (Santa Pola, Alicante, Spain). Tetramethyl orthosilicate (TMOS; purum, >98.0%) and Acrylamide (>99%) were purchased from Sigma-Aldrich, Inc. Hydrochloric Acid (12.1 M) was purchased from Aqua Solutions (Deer Park, TX). Sodium Chloride was purchased from Fisher Scientific Inc. and Tris[hydroxymethyl]aminomethane (Tris) was purchased from USB Corporation (Cleveland, OH). 1,2-Dimirystoyl-sn-glycero-3-phosphocholine (DMPC) in chloroform was purchased from Avanti Polar Lipids, Inc. Styrene-Maleic Acid (SMA) copolymer (Xiran SL 25010-P20) solution was obtained free of charge from Polyscope Polymers (Geleen, Netherlands). The styrene to maleic acid ratio was 3:1 and the molecular weight of the polymer was 4000 g/mol. The water used in all the experiments was purified using a Barnstead Nanopure Deionization System (Barnstead Thermolyne Corp., IA) and had a resistivity of 17.8 MΩ-cm or greater.

Silica Gel Synthesis. 15.2 ml of TMOS was added dropwise to a beaker in contact with an ice bath containing 11 ml of 0.002 M HCl solution. The mixture was then tip-sonicated for 15 minutes for the hydrolysis of the precursor. To remove the methanol produced during the hydrolysis reaction, the solution was rotary evaporated at 340 mbar vacuum pressure and 50℃ for 5-10 minutes. The final silica sol (pH~3) was obtained by filtering the remaining solution through a 0.22 um filter. To induce gelation, tris buffer (20mM Tris 100mM NaCl, pH 7.4) was mixed with the silica sol in various volumetric ratios in a methacrylate cuvette. The sol: buffer volumetric ratios were varied from 1:1 to 1:4 with the final volume of the gel monolith as 2.5 ml. Gelation typically occurred in 1-5 minutes with longer times for samples with larger amounts of buffer. For BR-PM encapsulation, lyophilized PM fragments were solubilized in DI water at a concentration

of 5 mg/ml and tip sonicated for 2-3 minutes to form a homogenous suspension. 62.5 ul of the PM stock solution (120 uM, 5 mg BR-PM/ml) was added to the desired buffer volume before it was mixed with sol to induce gelation. The final volume of the silica gel monolith was 2.5 ml and the final BR concentration was 3 μM. BR concentration was determined spectrophotometrically using the molar extinction coefficient of 62,700 M^{-1} cm^{-1} at 565 nm.

Synthesis of BR-DMPC-SMA Nanodiscs. We used a procedure which is similar to Orwick-Rydmerk et al. in order to form BR-DMPC-SMA Nanodiscs. Briefly, 800ul of DMPC stock solution in chloroform (25mg/ml) was dried under nitrogen and then stored under vacuum for at least 4 hours. The 20mg of dried DMPC lipid film was then hydrated with 1ml of 20mM Tris, 100mM NaCl, pH 7.4 buffer. 400ul of PM stock solution (5mg/ml) was centrifuged at 15000 rpm for one hour at room temperature. The pelleted PM was then solubilized with the 1 ml solution of hydrated DMPC vesicles. The PM-DMPC mixture was bath sonicated with heat for 45 minutes to form BR-DMPC vesicles (final temperature of 45-50°C). After cooling the solution to room temperature, 1 ml of SMA copolymer (Styrene: maleic acid ratio 1:3; 6mg/ml in 20mM Tris, 100mM NaCl, pH 7.4 buffer) was added dropwise to the solution to form BR-DMPC-SMA nanodiscs. The solution turned from cloudy to clear upon SMA addition. The final solution was again centrifuged at 15,000 rpm for 30 minutes to remove any insolubilized PM fragments. The supernatant containing BR-DMPC-SMA nanodiscs was collected and filtered through 0.22 um filter before further characterization.

Absorbance and Fluorescence Spectroscopy. UV-Visible absorbance spectroscopy of BR was used to determine the presence of retinal bound to a properly folded protein in solution and in silica gel. The absorbance measurements were performed using UV-2450 UV/vis spectrophotometer with temperature control (Shimadzu Corp., Kyoto, Japan). For dark-adapted spectra, samples were

kept in dark for 12 hours before recording the absorbance values. Samples were then irradiated under 100mW/cm white light for 10 minutes to record the light-adapted spectra. For BR-PM, temperature-dependent absorbance spectra were recorded between 300 and 700 nm with temperatures varying from 20℃ to 70℃ at a 10℃ interval for all samples typically containing 3μM BR. The samples were incubated at each temperature for 3 min before taking the measurement. For samples with BR-PM in silica, temperature-dependent absorbance spectra of blank silica gels were subtracted as references to get the final spectra. Absorbance spectra of BR nanodiscs in solution and in silica was recorded at temperatures between 30 °C and 70 °C at 5°C intervals at 3μM final BR concentration. The BR nanodisc in solution spectra were corrected by subtraction of DMPC-SMA nanodisc absorption at each temperature and BR nanodisc in silica was corrected by subtracting the blank silica gel absorbance with temperature. Difference spectrum for BR nanodiscs was then calculated using the corrected spectra by using the absorbance measured at 20 °C to quantify the extent of protein denaturation with increasing temperature.

Intrinsic fluorescence emission of tryptophan residues in BR was used to probe the changes in their local environment before and after encapsulation. The samples were excited at 295 nm and the emission spectra were recorded between 310 nm and 500 nm using a JASCO FP-8500 spectrophotometer (JASCO, Inc., Easton, MD). The excitation and emission slit-width was 2.5 nm and a response time of 0.5 seconds with a scan speed of 2000 nm/min. Temperature-dependent unfolding of the protein was studied by recording the tryptophan emission between 10℃ and 90℃. The samples were incubated at each temperature for 3 min before taking the measurements. The recorded maximum emission intensity (See Equation S1 and S2) at each temperature was then normalized with the initial maximum intensity at 10℃ for data analysis.

Acrylamide Quenching to Determine Tryptophan Accessibility. Accessibility of tryptophan residues to the solvent can be determined using Stern-Volmer plots derived using the theory of collisional fluorescence quenching. In these experiments, acrylamide was used to quench fluorescence from BR tryptophan residues. Acrylamide stock solution (4M) was added to 2.5 ml of BR-PM and BR-DMPC-SMA nanodiscs solution samples at 25 ul increments to achieve final acrylamide concentration of 0.20M (increments of 0.04M). The emission spectrum was recorded at each acrylamide concentration and the maximum fluorescence intensity was normalized with respect to the initial maximum emission intensity (no acrylamide). For silica gel samples encapsulating BR-PM and BR-DMPC-SMA nanodiscs, the gels were made with 0-0.20 M acrylamide and 3 uM BR. The samples were excited at 295 nm and the emission was recorded between 310 nm and 500 nm. The excitation and emission slit-width was 2.5 nm and a response time of 0.5 seconds with a scan speed of 2000 nm/min.

The obtained intensity data was plotted with respect to acrylamide concentration to obtain the Stern-Volmer plot and was fit to the Stern-Volmer Equation S1,

$$\text{(S1)} \quad \frac{F_0}{F} = 1 + K_s[Q]$$

Where F_0 is fluorescence emission in the absence of quencher and F is observed fluorescence emission at a known concentration [Q] of the quencher. K_s is the Stern-Volmer constant which indicates the relative accessibility of the tryptophan residues to the solvent.

Fluorescence Anisotropy. The fluorescence anisotropy of tryptophan residues in BR was measured to determine change in the rotational mobility of BR-PM fragments and BR-DMPC-SMA nanodiscs upon encapsulation in silica gels. The rotational speed of a fluorescent probe is inversely related to its size and can be represented with anisotropy value (r) of the emitted

fluorescence. Anisotropy can be described by the relationship between the intensity of the parallel ($F_{\parallel}$) and perpendicular ($F_{\perp}$) polarized light emission as shown in Equation S2,

$$\text{(S2)} \quad r = \frac{F_{\parallel} - GF_{\perp}}{F_{\parallel} + 2GF_{\perp}}$$

Here, G factor is the sensitivity ratio of the instrument towards horizontally and vertically polarized light. Tryptophan residues in both solution and gel samples were excited at 295 nm and the polarized light emission was recorded at 337 nm and 326 nm for BR-PM and BR-DMPC-SMA nanodiscs respectively. All fluorescence anisotropy measurements were recorded at 20 ℃.

S2. Bacteriorhodopsin Intrinsic Fluorescence Emission. BR Tryptophan residues were excited with a 295 nm wavelength and their emission spectrum was recorded between 310 and 500 nm. The raw spectrum was regressed using an empirically derived log-normal distribution. The Equation S3 for the log-normal distribution is shown below.

$$\text{(S3)} \quad F(\lambda) = \frac{h}{\frac{\lambda}{m} - \theta} * \exp\left[-\frac{(\ln\left(\frac{\lambda}{m} - \theta\right) - \mu)^2}{2\sigma^2}\right] + b$$

To determine the maximum emission wavelength, the derivative of Equation S4 can be set to zero such that,

$$\text{(S4)} \quad \lambda_{max} = m * \exp[\mu - \sigma^2] + \theta.$$

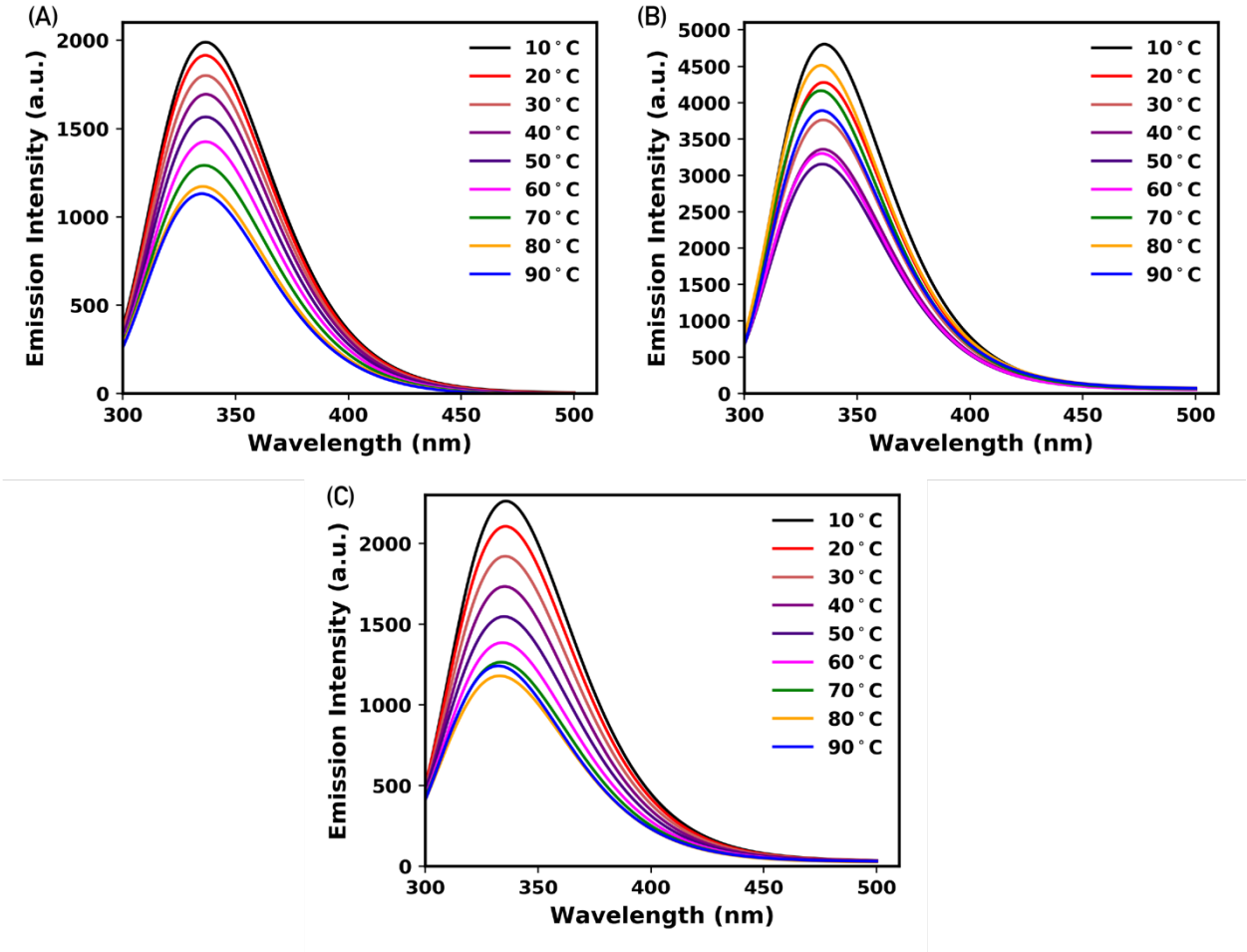

Figure S1. Temperature-dependent intrinsic fluorescence emission spectrum of BR-PM (A) in tris-HCl buffer solution (20mM tris, 100 mM NaCl, pH7.4) (B) in silica 1:1 (sol:buffer) and (C) in silica 1:4 (sol:buffer). The emission data shown is regressed from the raw data using eq S3.

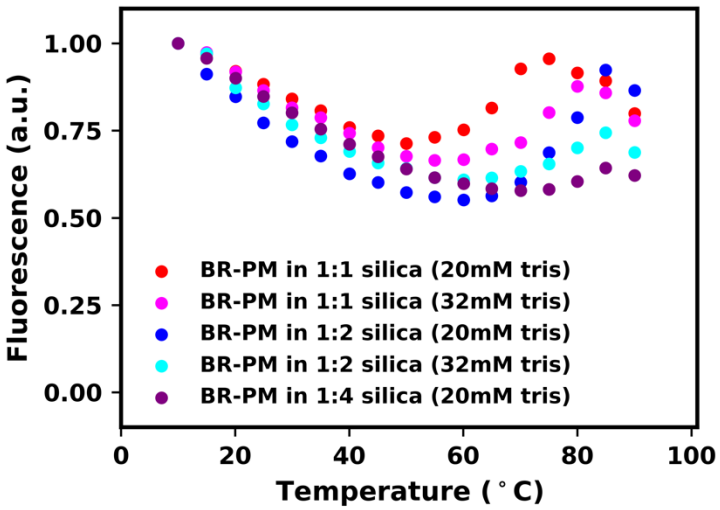

Figure S2. Intrinsic fluorescence emission of BR-PM in silica gels made with different sol:buffer volumetric ratios with increasing temperature. The buffer used in these experiments was 20mM Tris, 100mM NaCl, pH7.4 or 32 mM Tris, 100mM NaCl, pH7.4. The fluorescence emission intensity at 337 nm is normalized to the initial value measured at 10 °C for all samples.

S3. BR Nanodiscs Light-Dark Adaptation

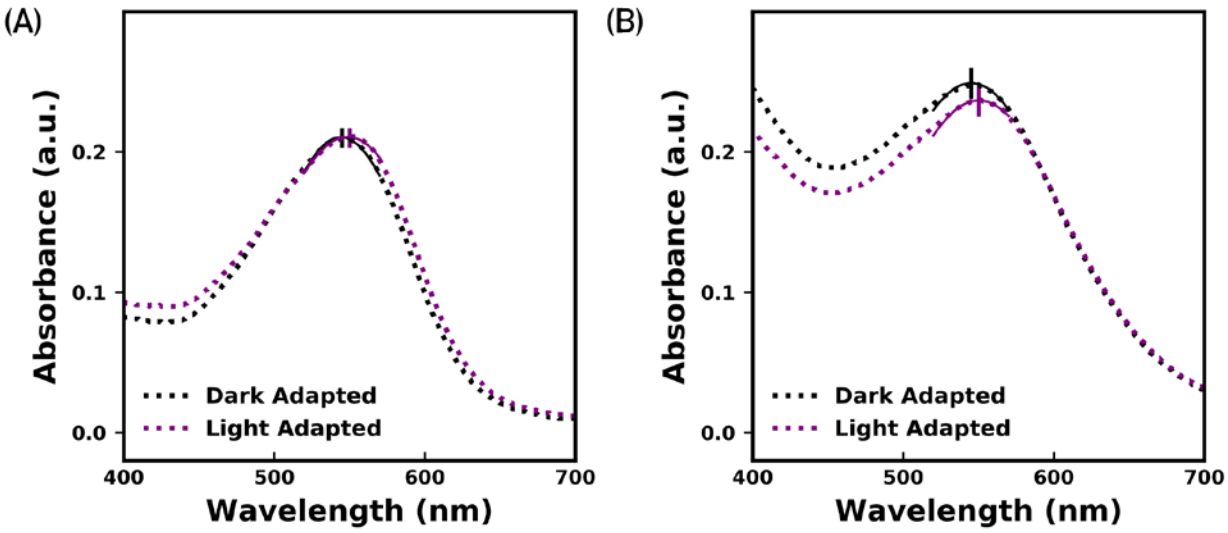

Figure S3. Room temperature steady-state UV-Visible absorbance spectrum of BR-DMPC-SMA nanodiscs in the dark and light adapted states in (A) 20 mM Tris 100 mM NaCl pH 7.4 buffer solution and (B) after encapsulation in silica gel monoliths synthesized with a 1:4 volumetric ratio of silica sol: buffer. The absorbance peaks are marked on the spectra for visualization of the red-shift that occurs upon light illumination.

S4. BR Nanodiscs Intrinsic Fluorescence Emission

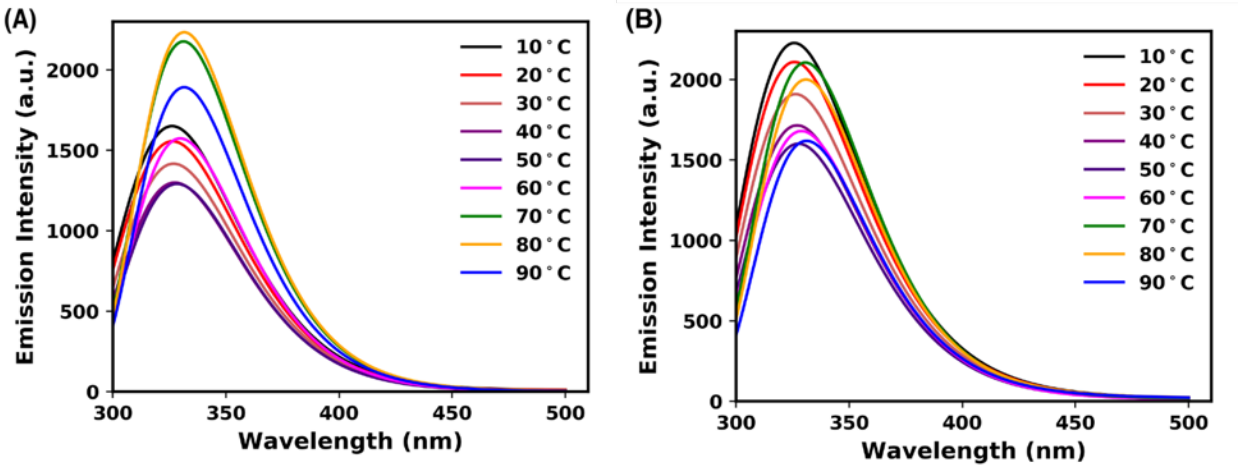

Figure S4. Temperature-dependent intrinsic fluorescence emission spectrum of BR nanodiscs in (A) tris-HCl buffer solution (20 mM tris, 100 mM NaCl, pH 7.4) and (B) in silica 1:4 (sol:buffer). The emission data is regressed from the raw data using eq S3.

S5. BR Nanodiscs UV-Visible Absorbance Spectrum.

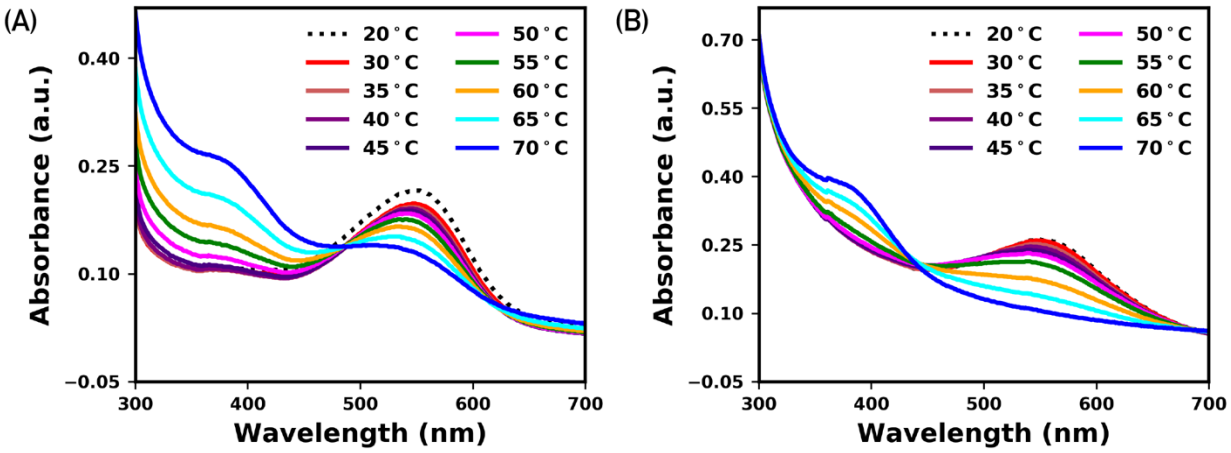

Figure S5. Temperature-dependent steady-state UV-Visible absorbance spectrum of BR-DMPC-SMA nanodiscs in (A) 20 mM Tris 100 mM NaCl pH 7.4 buffer solution and (B) after encapsulation in silica gel monoliths synthesized with a 1:4 volumetric ratio of silica sol: buffer.

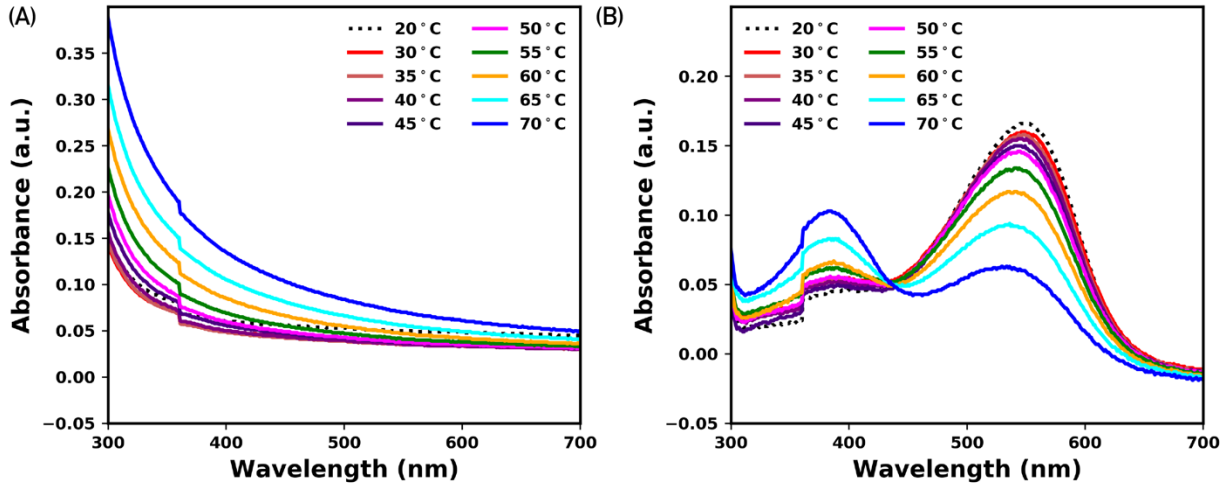

Figure S6. Temperature-dependent steady-state UV-Visible absorbance spectrum of (A) DMPC-SMA nanodiscs in 20 mM Tris 100 mM NaCl pH 7.4 buffer solution (B) BR-DMPC-SMA nanodiscs after subtracting the absorbance of DMPC-SMA nanodiscs at each temperature. The

absorbance observed between 300-350 nm in Figure S5 decreases upon removal of the background of SMA absorbance.

S6. Dynamic Light Scattering of DMPC-SMA-Nanodiscs

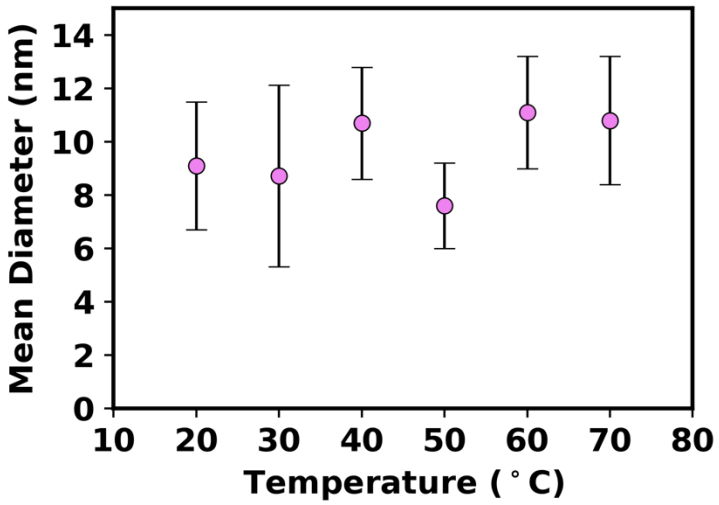

Figure S7. Mean diameter of DMPC-SMA nanodiscs with increasing temperature measured using dynamic light scattering. The error bars show the standard deviation of the particle sizes at each temperature.